

In the format provided by the authors and unedited.

## Room-temperature current blockade in atomically defined single-cluster junctions

Giacomo Lovat<sup>†</sup>, Bonnie Choi<sup>†</sup>, Daniel W. Paley, Michael L. Steigerwald, Latha Venkataraman\*  
& Xavier Roy\*

<sup>†</sup> These authors contributed equally to this work

\* Corresponding authors. E-mail: (L.V.) lv2117@columbia.edu; (X.R.) xr2114@columbia.edu

### **Table of Contents**

1. Synthetic details .....	2
2. Instrumentation.....	4
3. Single crystal x-ray diffraction.....	5
5. Crystal structures .....	8
6. Electrochemistry .....	10
7. Details of STM break-junction experiments.....	11
8. DFT calculations .....	13
9. References .....	13

## 1. Synthetic details

**General Information.** Chlorodiethylphosphine was purchased from Acros Organics. Dicobalt octacarbonyl and selenium powder were purchased from Strem Chemicals. All other reagents and solvents were purchased from Sigma Aldrich. Dry and deoxygenated solvents were prepared by elution through a dual-column solvent system (MBraun SPS). All reactions and sample preparations were carried out under inert atmosphere using standard Schlenk techniques or in a nitrogen-filled glovebox unless otherwise noted. Diethyl-4-(methylthio)phenyl phosphine (L) and  $\text{Co}_6\text{Se}_8\text{L}_6$  were prepared according to published protocol.<sup>1</sup>

### $\text{Co}_6\text{S}_8\text{L}_6$

The molecular cluster was prepared using a modified procedure for the synthesis of  $[\text{Co}_6\text{S}_8(\text{PEt}_3)_6][\text{BPh}_4]$  by Cecconi *et al.*<sup>2</sup> The ligand L (1.00 g, 4.71 mmol) was added to a degassed solution of  $\text{Co}(\text{BF}_4)_2 \cdot 6\text{H}_2\text{O}$  (530 mg, 1.57 mmol) in acetone/ethanol (1:1; 15 mL:15 mL). The mixture turned from pink to green-brown. Hydrogen sulfide was bubbled through the solution for 10 mins at room temperature. During that time, the reaction turned dark brown. The mixture was stirred for 16 h under nitrogen. The black precipitate that formed was collected on a glass frit, washed with a small amount of acetone/ethanol and dried *in vacuo*.  $^1\text{H}$  NMR shows that the solid contains only  $\text{Co}_6\text{S}_8\text{L}_6$ . The product was recrystallized by slow evaporation of a concentrated dichloromethane solution under inert atmosphere. Yield: 25 mg (5 %)

$^1\text{H}$  NMR (400 MHz,  $[\text{d}_2\text{-dichloromethane}]$ , 298 K):  $\delta = 0.87$  (6H, m), 1.95 (4H, m), 2.49 (3H, s), 7.14 (2H, d), 7.30 (2H, t).

### $[\text{Co}_6\text{S}_8\text{L}_6][\text{BF}_4]$

When we expose the acetone/ethanol filtrate from the  $\text{Co}_6\text{S}_8\text{L}_6$  synthesis to air for several days, black block-like crystals of  $[\text{Co}_6\text{S}_8\text{L}_6][\text{BF}_4]$  form in the solution. The product was recrystallized by diffusing ethanol into a concentrated solution of  $[\text{Co}_6\text{S}_8\text{L}_6][\text{BF}_4]$  in dichloromethane. The crystals were collected, rinsed with ethanol and dried *in vacuo*. Yield: 180 mg (35 %).

$^1\text{H}$  NMR (400 MHz,  $[\text{d}_2\text{-dichloromethane}]$ , 298 K):  $\delta = -2.68$  (4H, br),  $-0.08$  (6H, br s), 2.48 (3H, s), 6.98 (2H, d), 7.33 (2H, m).

**[Co<sub>6</sub>S<sub>8</sub>L<sub>6</sub>][BF<sub>4</sub>]<sub>2</sub>**

A solution of AgBF<sub>4</sub> (5 mg, 24 μmol) in 0.2 mL of acetonitrile was added dropwise to a solution of Co<sub>6</sub>S<sub>8</sub>L<sub>6</sub> (21 mg, 11 μmol) in 3 mL of dichloromethane. The vial was wrapped in foil to protect the reaction from light and stirred 16 h. The solvent was removed *in vacuo* and 5 mL of dichloromethane was added to the crude product. The mixture was filtered through a 0.2 μm syringe filter and the solvent was removed *in vacuo*. The solid was dissolved in 0.5 mL of acetonitrile and the resulting dark brown solution was layered over toluene (10 mL). Dark brown crystals of [Co<sub>6</sub>S<sub>8</sub>L<sub>6</sub>][BF<sub>4</sub>]<sub>2</sub> were obtained after 5 days at -35 °C. The crystals were collected, rinsed with toluene and hexanes, and dried *in vacuo*. Yield: 16 mg (70 %).

<sup>1</sup>H NMR (400 MHz, [CD<sub>3</sub>CN], 298 K): δ = -4.47 (4H, br), -1.28 (6H, br s), 2.34 (3H, s), 6.78 (2H, d), 8.02 (2H, m).

**[Co<sub>6</sub>Se<sub>8</sub>L<sub>6</sub>][BF<sub>4</sub>]**

A solution of ferrocenium tetrafluoroborate (9 mg, 44 μmol) in 4 mL of acetonitrile was added dropwise to a solution of Co<sub>6</sub>Se<sub>8</sub>L<sub>6</sub><sup>1</sup> (72 mg, 44 μmol) in 4 mL of tetrahydrofuran. The reaction was stirred 16 h. The solvent was removed *in vacuo* and the solid was rinsed with toluene. The product was dissolved in 2 mL of acetonitrile and the solution was filtered through a 0.2 μm syringe filter. The mixture was concentrated *in vacuo* and layered over toluene (5 mL). Dark brown crystals of [Co<sub>6</sub>Se<sub>8</sub>L<sub>6</sub>][BF<sub>4</sub>] were obtained after 5 days at -35 °C. The crystals were collected, rinsed with toluene and hexanes, and dried *in vacuo*. Yield: 30 mg (40 %)

<sup>1</sup>H NMR (400 MHz, [d<sub>2</sub>-dichloromethane], 298 K): δ = -1.44 (4H, br), 0.00 (6H, br s), 2.51 (3H, s), 6.90 (2H, d), 7.16 (2H, m).

**[Co<sub>6</sub>Se<sub>8</sub>L<sub>6</sub>][BF<sub>4</sub>]<sub>2</sub>**

A solution of ferrocenium tetrafluoroborate (15 mg, 53 μmol) in 4 mL of acetonitrile was added dropwise to a solution of Co<sub>6</sub>Se<sub>8</sub>L<sub>6</sub><sup>1</sup> (60 mg, 26 μmol) in 4 mL of tetrahydrofuran. The reaction was stirred 16 h. The solvent was removed *in vacuo* and the solid was rinsed with toluene. The product was dissolved in 2 mL of acetonitrile and the resulting solution was filtered through a 0.2 μm syringe filter. The mixture was concentrated *in vacuo* and layered over toluene (5 mL). Dark brown crystals of [Co<sub>6</sub>Se<sub>8</sub>L<sub>6</sub>][BF<sub>4</sub>]<sub>2</sub> were obtained after 2 days. The crystals were collected, rinsed with toluene and hexanes, and dried *in vacuo*. Yield: 32 mg (50 %)

**<sup>1</sup>H NMR** (400 MHz, [d<sub>2</sub>-dichloromethane], 298 K):  $\delta$  = -5.26 (4H, br), -0.76 (6H, br s), 2.43 (3H, s), 6.58 (2H, d), 7.74 (2H, m).

## 2. Instrumentation

### *NMR*

All <sup>1</sup>H NMR were recorded on a Bruker DRX400 (400 MHz) spectrometer.

### *x-ray diffraction*

Single crystal x-ray diffraction data were collected on an Agilent SuperNova diffractometer using mirror-monochromated Cu K $\alpha$  or Mo K $\alpha$  radiation. Data collection, integration, scaling (ABSPACK) and absorption correction (face-indexed Gaussian integration<sup>3</sup> or numeric analytical methods<sup>4</sup>) were performed in CrysAlisPro.<sup>5</sup> Structure solution was performed using ShelXT.<sup>6</sup> Subsequent refinement was performed by full-matrix least-squares on F<sup>2</sup> in ShelXL.<sup>6</sup> Olex2<sup>7</sup> was used for viewing and to prepare CIF files. Many disordered molecules (e.g. BF<sub>4</sub> anions) were modeled as rigid fragments from the Idealized Molecular Geometry Library.<sup>8</sup> ORTEP graphics were prepared in CrystalMaker.<sup>9</sup> Thermal ellipsoids are rendered at the 50% probability level. Details of crystallographic data and parameters for data collection and refinement are in Table S1.

Crystals were mounted on MiTeGen mounts with the aid of Parabar oil and cooled to 100 K on the diffractometer for screening and data collection. A minimum of 1 hemisphere of data to 0.8 Å resolution was collected for all compounds.

### *ex situ cyclic voltammetry*

Electrochemistry was carried out in dichloromethane or acetonitrile with tetra-*n*-butylammonium hexafluorophosphate (TBAPF<sub>6</sub>) supporting electrolyte (0.1 M) using a Princeton Applied Research PARSTAT 2263 potentiostat inside an argon-filled glovebox. Measurements were carried out with a glassy carbon working electrode, a platinum counter electrode, and a silver pseudo-reference electrode. Measurements were calibrated using the ferrocene/ferrocenium redox couple.

### 3. Single crystal x-ray diffraction

Structure solution and space group assignment were performed in ShelXT with no difficulty. In the final refinements, non-H atoms were refined anisotropically with no restraints unless noted; C-H hydrogens were placed in calculated positions and refined with riding isotropic ADPs and coordinates. The non-routine details of the refinements are given below:

#### **Co<sub>6</sub>S<sub>8</sub>L<sub>6</sub>**

One C<sub>6</sub>H<sub>4</sub>SMe group was disordered over two positions, which were located with the aid of rigid phenyl fragments (AFIX 66) and subsequently refined with SAME and RIGU restraints. All other details of the refinement were routine.

#### **[Co<sub>6</sub>S<sub>8</sub>L<sub>6</sub>][BF<sub>4</sub>] and [Co<sub>6</sub>Se<sub>8</sub>L<sub>6</sub>][BF<sub>4</sub>]**

These structures are isostructural and were solved and refined routinely in P-1.

#### **[Co<sub>6</sub>S<sub>8</sub>L<sub>6</sub>][BF<sub>4</sub>]<sub>2</sub>**

There are two independent clusters, one with 1/6 molecule in the asymmetric unit and the other with 1/3 molecule in the asymmetric unit. These were each refined routinely; one disordered ethyl group on the phosphine was modeled in two independent positions with SAME and RIGU restraints to stabilize its geometry and ADPs.

There are three independent BF<sub>4</sub> molecules, all disordered over different symmetry elements. One BF<sub>4</sub> sits on a twofold axis (Wyckoff site *f*) with a whole molecule in the asymmetric unit; this was placed in PART -1 with occupancy 1/2. Another BF<sub>4</sub> is on a threefold axis (Wyckoff site *d*) with 1/3 molecule in the asymmetric unit; this molecule is additionally disordered in a 90:10 ratio by a non-crystallographic inversion center. The final BF<sub>4</sub> is on Wyckoff site *a* (site symmetry 32) and fulfills the symmetry of the threefold axis but not the perpendicular twofold axis. The necessary special position constraints were set up by hand: for the B atom and the F sitting on the threefold axis,  $x = y = 0$ ;  $U^{11} = U^{22}$ ;  $U^{23} = U^{13} = 0$ ;  $U^{12} = 1/2 * U^{11}$ .

All 1,2 B-F distances and 1,3 F-F distances were made equivalent with a floating DFIX restraint. The ADPs of two of the disordered BF<sub>4</sub> anions were restrained with RIGU. ADPs of overlapping atoms were stabilized with a short-range SIMU restraint.

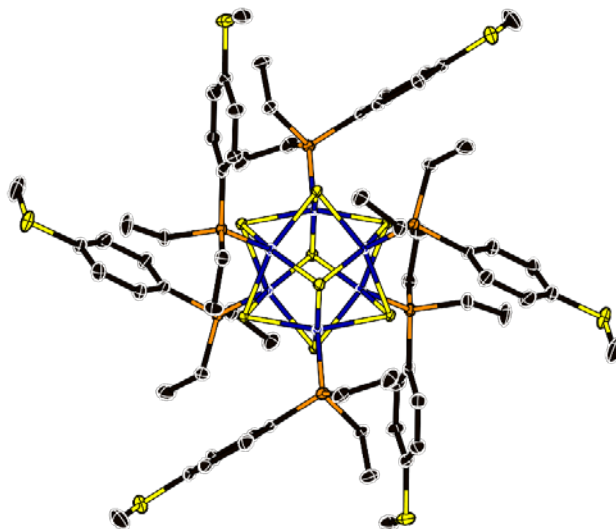
**[Co<sub>6</sub>Se<sub>8</sub>L<sub>6</sub>][BF<sub>4</sub>]<sub>2</sub>**

This crystal is isostructural with [Co<sub>6</sub>S<sub>8</sub>L<sub>6</sub>][BF<sub>4</sub>]<sub>2</sub> and the coordinates from the previous solution were used directly instead of solving de novo. All details of the refinement were identical, except that the disorders of the L ethyl group and the BF<sub>4</sub> on Wyckoff site *d* were not observed.

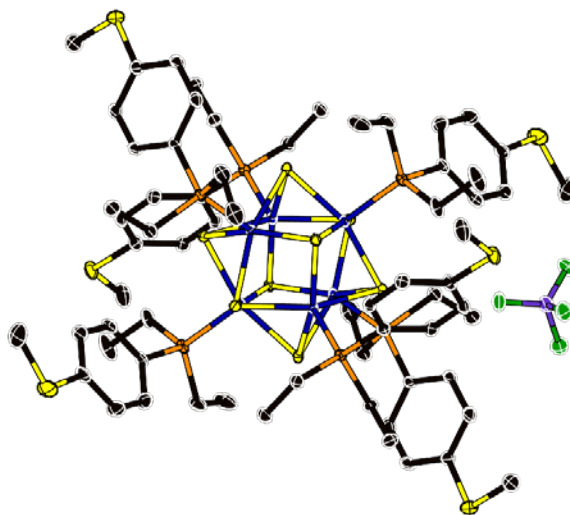
Supplementary Table 1. Selected crystallographic data.

Compound	Co <sub>6</sub> S <sub>8</sub> L <sub>6</sub>	[Co <sub>6</sub> S <sub>8</sub> L <sub>6</sub> ][BF <sub>4</sub> ]	[Co <sub>6</sub> S <sub>8</sub> L <sub>6</sub> ][BF <sub>4</sub> ] <sub>2</sub>	[Co <sub>6</sub> Se <sub>8</sub> L <sub>6</sub> ][BF <sub>4</sub> ]	[Co <sub>6</sub> Se <sub>8</sub> L <sub>6</sub> ][BF <sub>4</sub> ] <sub>2</sub>
Formula	C <sub>66</sub> H <sub>102</sub> Co <sub>6</sub> S <sub>14</sub> P <sub>6</sub>	C <sub>66</sub> H <sub>102</sub> Co <sub>6</sub> S <sub>14</sub> P <sub>6</sub> BF <sub>4</sub>	C <sub>66</sub> H <sub>102</sub> Co <sub>6</sub> S <sub>14</sub> P <sub>6</sub> B <sub>2</sub> F <sub>8</sub>	C <sub>66</sub> H <sub>102</sub> Co <sub>6</sub> Se <sub>8</sub> P <sub>6</sub> BF <sub>4</sub>	C <sub>66</sub> H <sub>102</sub> Co <sub>6</sub> Se <sub>8</sub> P <sub>6</sub> B <sub>2</sub> F <sub>8</sub>
MW	1883.71	1970.52	2057.33	2345.72	2432.53
Space group	I2/a	P-1	P-3c1	P-1	P-3c1
<i>a</i> (Å)	21.3182(2)	12.9224(3)	21.0803(3)	12.9605(8)	21.0332(4)
<i>b</i> (Å)	16.8028(1)	13.9345(3)	21.0803(3)	14.1401(8)	21.0332(4)
<i>c</i> (Å)	23.1835(3)	14.8239(3)	33.4515(5)	14.9645(9)	33.7301(9)
<i>α</i> (°)	90	114.2610(18)	90	115.457(6)	90
<i>β</i> (°)	103.849(1)	94.1899(17)	90	93.607(5)	90
<i>γ</i> (°)	90	114.823(2)	120	115.410(6)	120
<i>V</i> (Å <sup>3</sup> )	8063.05(14)	2109.23(9)	12873.6(4)	2131.3(3)	12922.9(6)
<i>Z</i>	4	1	6	1	6
$\rho_{\text{calc}}$ (g cm <sup>-3</sup> )	1.552	1.551	1.592	1.828	1.875
<i>T</i> (K)	100	100	100	100	100
$\lambda$ (Å)	1.54184	1.54184	1.54184	0.71073	1.54184
<b>2θ</b> <sub>min</sub> , <b>2θ</b> <sub>max</sub>	6.564, 146.002	6.85, 145.968	7.168, 146.452	6.882, 52.744	7.144, 146.964
<i>N</i> <sub>ref</sub>	75385	68304	164775	16049	237515
<b>R</b> (int), <b>R</b> ( $\sigma$ )	0.0608, 0.0318	0.0554, 0.0265	0.1668, 0.0516	0.0400, 0.0716	0.2002, 0.0528
$\mu$ (mm <sup>-1</sup> )	14.251	13.716	13.578	4.862	15.580
<i>T</i> <sub>max</sub> , <i>T</i> <sub>min</sub>	0.981, 0.970	0.759, 0.493	0.963, 0.919	0.975, 0.954	0.985, 0.962
<b>Data</b>	8036	8409	8592	8662	8622
<b>Restraints</b>	197	0	115	0	46
<b>Parameters</b>	498	466	535	466	501
<b>R</b> <sub>1</sub> (obs)	0.0291	0.0391	0.0614	0.0385	0.0852
<b>wR</b> <sub>2</sub> (all)	0.0666	0.1050	0.1693	0.0653	0.2215
<b>S</b>	1.024	1.026	1.006	1.015	1.066
<b>Peak, hole</b> (e <sup>-</sup> Å <sup>-3</sup> )	0.53, -0.46	0.95, -0.94	1.03, -0.83	0.69, -0.62	1.82, -1.33
<b>CCDC #</b>	1557952	1557951	1557954	1557950	1557953

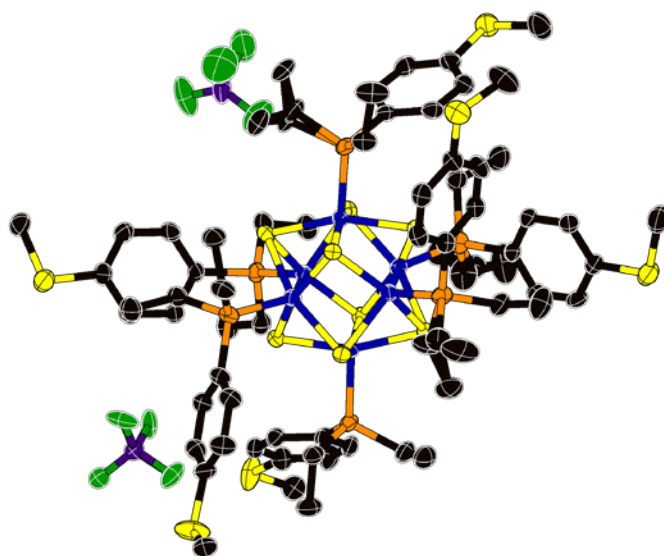
## 5. Crystal Structures



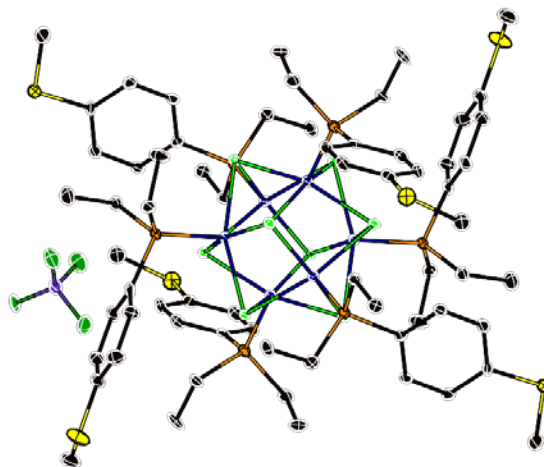
**Supplementary Fig. 1.** Crystal structure of  $\text{Co}_6\text{S}_8\text{L}_6$  showing thermal ellipsoids at 50% probability. Blue, cobalt; yellow, sulfur; orange, phosphorus; black, carbon. Hydrogen atoms were removed to clarify the view.



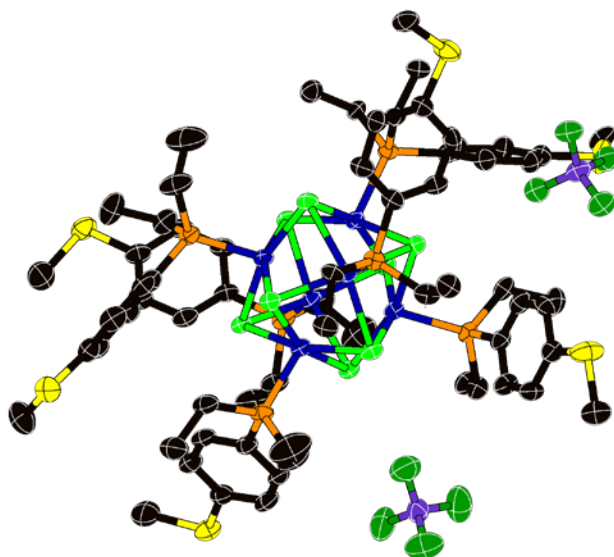
**Supplementary Fig. 2.** Crystal structure of  $[\text{Co}_6\text{S}_8\text{L}_6][\text{BF}_4]$  showing thermal ellipsoids at 50% probability. Blue, cobalt; yellow, sulfur; orange, phosphorus; black, carbon; purple, boron; green, fluorine. Hydrogen atoms were removed to clarify the view.



**Supplementary Fig. 3.** Crystal structure of  $[\text{Co}_6\text{S}_8\text{L}_6][\text{BF}_4]_2$  showing thermal ellipsoids at 50% probability. Blue, cobalt; yellow, sulfur; orange, phosphorus; black, carbon; purple, boron; green, fluorine. Hydrogen atoms were removed to clarify the view.

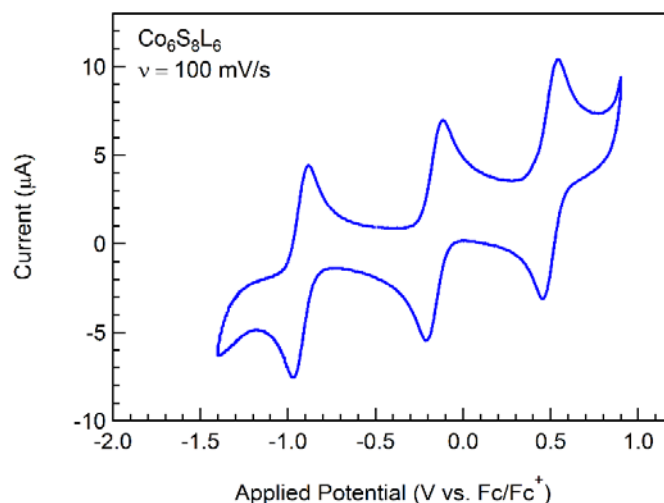


**Supplementary Fig. 4.** Crystal structure of  $[\text{Co}_6\text{Se}_8\text{L}_6][\text{BF}_4]$  showing thermal ellipsoids at 50% probability. Blue, cobalt; light green, selenium; yellow, sulfur; orange, phosphorus; black, carbon; purple, boron; green, fluorine. Hydrogen atoms were removed to clarify the view.

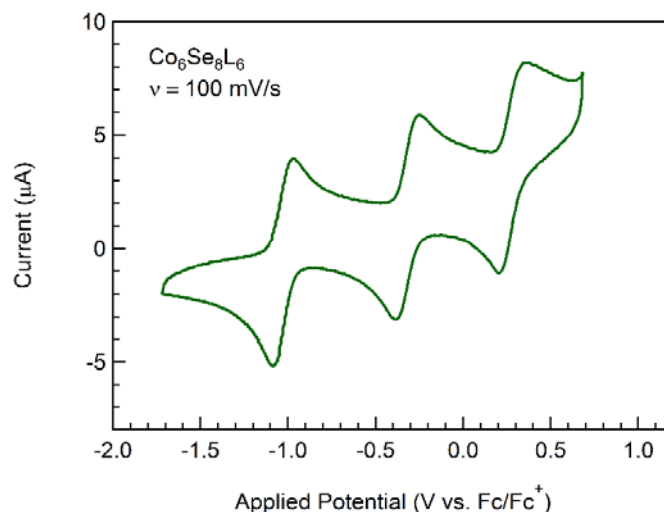


**Supplementary Fig. 5.** Crystal structure of  $[\text{Co}_6\text{Se}_8\text{L}_6][\text{BF}_4]_2$  showing thermal ellipsoids at 50% probability. Blue, cobalt; light green, selenium; yellow, sulfur; orange, phosphorus; black, carbon; purple, boron; green, fluorine. Hydrogen atoms were removed to clarify the view.

## 6. Electrochemistry



**Supplementary Fig. 6.** Cyclic voltammogram of  $\text{Co}_6\text{S}_8\text{L}_6$  in 0.1 M  $\text{TBAPF}_6$  in dichloromethane with a 100 mV/s scan rate.

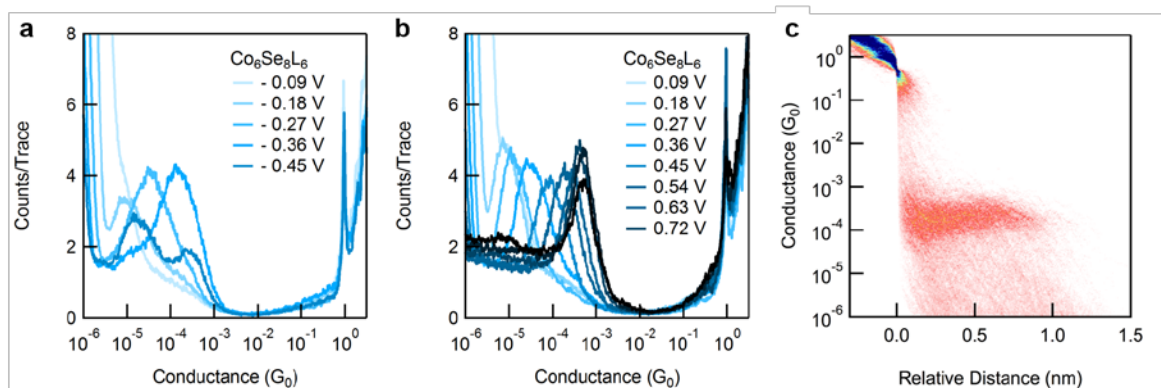


**Supplementary Fig. 7.** Cyclic voltammogram of  $\text{Co}_6\text{Se}_8\text{L}_6$  in 0.1 M  $\text{TBAPF}_6$  in dichloromethane with a 100 mV/s scan rate.

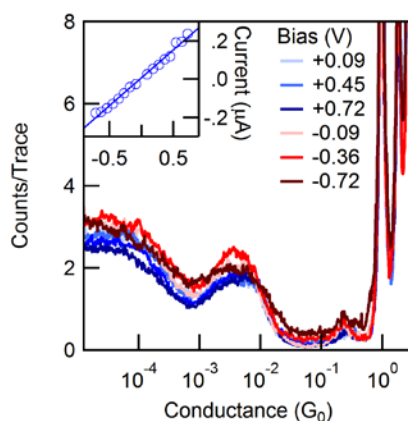
## 7. Details of STM break-junction experiments

**Experimental Procedure.** We measured the conductance of single-molecule junctions formed with two gold electrodes using a home-built modified Scanning Tunneling Microscope (STM). We used 0.25 mm diameter cut gold wire (99.95%, Alfa Aesar) as the STM tips and 100 nm gold-coated (99.999%, Alfa Aesar) steel pucks as substrates. A commercially available single-axis piezoelectric positioner (Nano-P15, Mad City Labs) was used to achieve sub-angstrom level control of the tip-substrate distance. The STM was controlled using a custom written program in IgorPro (Wavemetrics, Inc.) and operated in ambient conditions at room temperature. The gold substrates were cleaned using a UV/ozone cleaning lamp for 20 minutes prior to use. For each measurement, 1000 traces were first collected prior to adding molecular solutions to check the cleanliness of the gold surface. Solutions of the target molecules at  $\sim 10 \mu\text{M}$  concentration in propylene carbonate (Alfa Aesar, 99% purity) were added to the substrate for STM break-junction measurements at applied biases ranging from  $\pm 0.1$  to  $\pm 1$  V. After the formation of each Au-Au junction, the piezoelectric motor moved the substrate at a speed of 20 nm/s to break the junction. The current and voltage data were acquired at 40 kHz. For each of the compounds,  $\text{Co}_6\text{Se}_8\text{L}_6$  and  $\text{Co}_6\text{S}_8\text{L}_6$ , we collected 1,000 traces at each bias to generate 1D and 2D conductance histograms without data selection (see Supplementary Fig. 8).

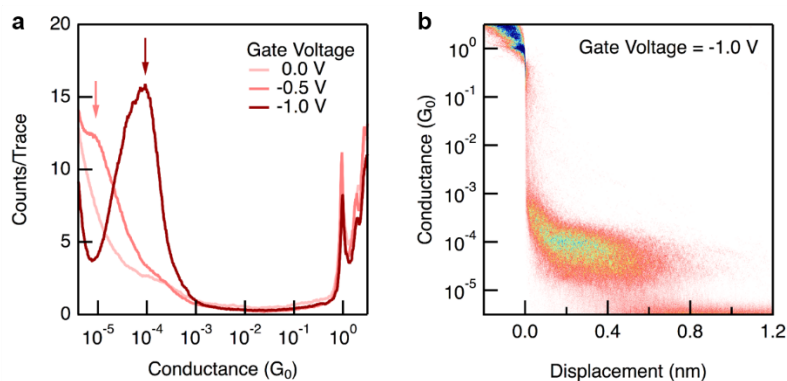
For the three-electrode measurements (Supplementary Fig. 10), a Pt wire was inserted into the PC solution (in addition to the tip and substrate) and the voltage at the Pt wire was controlled using a separate output channel of the data acquisition card, thereby working as a gate electrode.<sup>10</sup> Measurements were done with an added electrolyte (100 mM tetrabutylammonium perchlorate). The tip/substrate bias was set to 90 mV and the potential on the Pt wire was varied during the measurement. Conductance histograms of 1000 traces measured at different gate potentials were recorded and are presented in Supplementary Fig. 10.



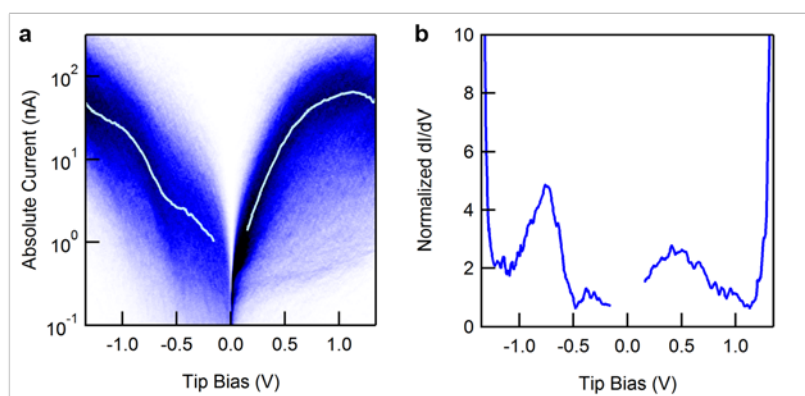
**Supplementary Fig. 8.** **a,b**, 1D conductance histograms of  $\text{Co}_6\text{Se}_8\text{L}_6$  measured at different tip biases in PC using STM-BJ technique. **c**, 2D histogram measured at -450 mV.



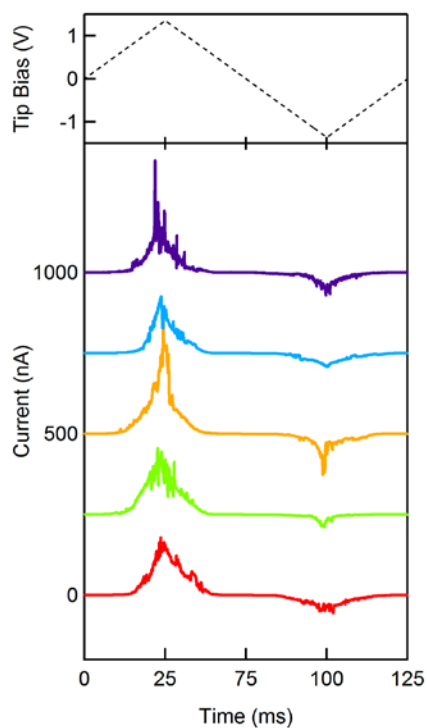
**Supplementary Fig. 9.** 1D conductance histograms of ligand L measured at different tip biases in PC using STM-BJ technique. The inset presents the current as a function of tip bias and shows a clear linear trend.



**Supplementary Fig. 10.** **a**, 1D conductance histogram of  $\text{Co}_6\text{S}_8\text{L}_6$  measured at different gate voltages using a three-electrode setup. Depending on the gate voltage, conductance is turned on or off (e.g., trace at -1.0 V when conductance is turned on and at 0.0 V when conductance is turned off). **b**, 2D conductance histogram of  $\text{Co}_6\text{S}_8\text{L}_6$  at a gate voltage of -1.0 V.



**Supplementary Fig. 11.** **a**, I-V 2D histogram for  $\text{Co}_6\text{Se}_8\text{L}_6$ . The current axis is logarithmically binned. The superimposed white curve represents an average of the current over all traces per voltage bin. Note that the data between -0.2 V and 0.2 V includes some additional contributions due to capacitive currents as the voltage is swept at a rate of 50 V/s. **b**, Normalized differential conductance,  $dI/dV$ , extracted from the average I-V curve.



**Supplementary Fig. 12.** Sample traces of I-V measurement for  $\text{Co}_6\text{S}_8\text{L}_6$ .

## 8. DFT calculations

All calculations were done using Jaguar (Schrodinger, Inc., New York, NY, 2014). All calculations were based on density functional theory and used the B3LYP functional. The 6-31G\*\* basis sets were used throughout, with the LACVP potentials/basis sets used for the heavy atoms. The geometry of  $\text{trans-Co}_6\text{Se}_8[\text{P}(\text{CH}_3)_3]_4\text{L}_2$ , where  $\text{L} = \text{P}(\text{CH}_3)_2(\text{C}_6\text{H}_4\text{SCH}_3)$  was optimized; coordinates for this optimized geometry are available on request.

## 9. References

1. Roy, X. *et al.* Quantum soldering of individual quantum dots. *Angew. Chem. Int. Ed.* **51**, 12473-12476 (2012).
2. Cecconi, F., Ghilardi, C. A. & Midollini, S. Synthesis and structural characterization of a paramagnetic octahedral cobalt-sulfur cluster,  $[\text{Co}_6(\mu_3\text{-S})_8(\text{PEt}_3)_6]\text{BPh}_4$ . *Inorg. Chim. Acta* **64**, L47-48 (1982).
3. Blanc, E., Schwarzenbach, D. & Flack, H. D. The evaluation of transmission factors and their first derivatives with respect to crystal shape parameters. *J. Appl. Crystallogr.* **24**, 1035-1041 (1991).
4. Clark, R. C. & Reid, J. S. The analytical calculation of absorption in multifaceted crystals. *Acta Crystallogr.* **A51**, 887-897 (1995).
5. Version 1.171.37.35. Oxford Diffraction / Agilent Technologies UK Ltd, Yarnton, England (2014).
6. Sheldrick, G. M. SHELXT - Integrated space-group and crystal structure determination. *Acta Crystallogr.* **A71**, 3-8 (2015).
7. Dolomanov, O. V., Bourhis, L. J., Gildea, R. J., Howard, J. A. K. & Puschmann, H. OLEX2: A complete structure solution, refinement and analysis program. *J. Appl. Crystallogr.* **42**, 339-341 (2009).
8. Guzei, I. A. An idealized molecular geometry library for refinement of poorly behaved molecular fragments with constraints. *J. Appl. Crystallogr.* **47**, 806-809 (2014).
9. CrystalMaker Software Ltd, Oxford, England ([www.crystallmaker.com](http://www.crystallmaker.com)).
10. Capozzi, B. *et al.* Tunable charge transport in single-molecule junctions via electrolytic gating. *Nano Lett.* **14**, 1400-1404 (2014).